HHS Public Access

Author manuscript

Circ Res. Author manuscript; available in PMC 2017 January 08.

Published in final edited form as:

Circ Res. 2016 January 8; 118(1): 48–55. doi:10.1161/CIRCRESAHA.115.307767.

Uncoupling Caveolae from Intracellular Signaling In Vivo

Jan R. Kraehling[1,2], **Zhengrong Hao**[1,2], **Monica Y. Lee**[1,2], **David J. Vinyard**[3], **Heino Velazquez**[4], **X. Liu**[5], **Radu V. Stan**[6], **Gary W. Brudvig**[3], and **William C. Sessa**[1,2]

[1]Vascular Biology and Therapeutics Program, Yale University School of Medicine, New Haven, CT 06520, USA

[2]Department of Pharmacology, Yale University, School of Medicine, New Haven, CT 06520, USA

[3]Department of Chemistry, Yale University, New Haven, CT 06520, USA

[4]Department of Internal Medicine, VA Connecticut Healthcare System, West Haven, CT 06516, USA

[5]Department of Cell Biology, Yale University, School of Medicine, New Haven, CT 06520, US

[6]Department of Pathology, Dartmouth Medical School, Lebanon, NH 03756, USA

Abstract

Rationale—Caveolin-1 negatively regulates eNOS derived NO production and this has been mapped to several residues on Cav-1 including F92. Herein, we reasoned that endothelial expression of an F92ACav-1 transgene would let us decipher the mechanisms and relationships between caveolae structure and intracellular signaling.

Objective—This study was designed to separate caveolae formation from its downstream signaling effects.

Methods and Results—An endothelial-specific doxycycline-regulated mouse model for the expression of Cav-1-F92A was developed. Blood pressure by telemetry and nitric oxide bioavailability by electron paramagnetic resonance and phosphorylation of VASP were determined. Caveolae integrity in the presence of Cav-1-F92A was measured by stabilization of Cav-2, sucrose gradient and electron microscopy. Histological analysis of heart and lung, echocardiography and signaling were performed.

Conclusions—This study shows that mutant Cav-1-F92A forms caveolae structures similar to WT but leads to increases in NO bioavailability in vivo thereby demonstrating that caveolae formation and downstream signaling events occur through independent mechanisms.

Keywords

Caveolin-1; nitric oxide; eNOS; vascular function; endothelial cell; cell; mice

Address correspondence to: Dr. William C. Sessa, Vascular Biology and Therapeutics Program, Yale University School of Medicine, 10 Amistad Street, New Haven, CT 06520, USA, Tel: +1-203-737-2291, Fax: +1-203-737-2290, william.sessa@yale.edu.

DISCLOSURES

The authors declare that there are no conflicts of interest. The sponsors had no role in study design, data collection and analysis, decision to publish, or preparation of the manuscript.

INTRODUCTION

Caveolae organelles are flask shaped invaginations of the plasma membrane implicated in a variety of biological processes including endocytosis, transcytosis, mechano-sensing and signaling.[1–3] Caveolin-1 (Cav-1) is the main coat protein of caveolae in endothelial cells and is essential for the formation of caveolae[4]. Despite the critical role of Cav-1 in caveolae assembly, Cav-1 KO mice are viable and fertile, but show several cardiovascular and pulmonary phenotypes. Cav-1 KO mice exhibit impaired mechanosignaling and remodeling, myocardial hypertrophy, metabolic imbalances with elevated plasma lipids, pulmonary fibrosis and hypertension and are protected from atherosclerosis.[5–10] The precise mechanisms of how Cav-1 regulates these diverse phenotypes are unknown and most data are rationalized based on the critical role of Cav-1 in caveolae formation and mechanosignaling or via Cav-1 serving as a scaffolding protein integrating extracellular signaling pathways to intracellular effectors such as protein kinase A[11], G protein-coupled receptors[2, 12], Rab5[13] and endothelial nitric oxide synthase (eNOS)[14].

eNOS derived nitric oxide (NO) in the vascular system, is a major regulator of vascular tone and therefore blood pressure. eNOS is post-translationally palmitoylated and trafficked to caveolae[15], where its activity is decreased due to the binding to Cav-1.[14, 16] Domain mapping studies, revealed the aa 82 – 101 of Cav-1 are critical for Cav-1 interacting with eNOS[14, 16], whereas the aa T90, T91 and in particular F92 play a crucial role in the inhibitory action of this binding. After activation, eNOS is thought to be released from the inhibitory clamp of Cav-1 and phosphorylated by kinases including Akt[17]. Hsp90 and calmodulin binding leads to a fully activated eNOS[18], resulting in increased NO release. A hallmark of many vascular and pulmonary diseases is a decrease in the NO biogenesis or bioavailability via uncoupling. Therefore, understanding how to selectively activate eNOS could be beneficial.

Here, we report that inducible expression of a single point mutant of Cav-1 (Cav-1-F92A) in endothelium decreases systolic blood pressure. The reduction in blood pressure occurs contemporaneously with enhanced levels of NO bioactivity. Moreover, Cav-1-F92A does not interfere with the formation of caveolae or promote pulmonary fibrosis, myocardial dysfunction or hypertrophy, as seen in global Cav-1 KO mice. These data suggest that it is feasible to uncouple caveolae formation from its intracellular partners and disrupting the inhibitory interaction between Cav-1 and eNOS could be a potential therapeutic approach.

METHODS

Because of space limitations, a detailed description of the Materials and Methods is presented in the Online Data Supplement.

RESULTS

Endothelial specific expression of Cav-1-F92A

Previous studies have shown that Cav-1-F92A expression in endothelial cells (EC) leads to an increased nitric oxide (NO) release[19, 20]. To further investigate this Cav-1 point mutation

in EC in vivo, we generated an endothelial specific, doxycycline-controlled F92A Cav-1 transgenic mouse using a Cdh5-tTA driver line[21] bred to a tetracycline responsive element (TRE) driven F92A Cav-1 construct tagged with the HA epitope on its C terminus (Figure IA). The HA-tag was necessary to distinguish endogenous Cav-1 from transgenic Cav-1 as the Cav-1 antibody does not discriminate between human and murine proteins. The expression of Cav-1-F92A was confirmed in whole lung lysates by immunoblotting (Figure 1A). The endothelial specific expression was shown by isolating mouse lung endothelial cells (MLECs) using CD31 beads. The fractions bound to the beads ($CD31^+$) and the non-bound fraction ($CD31^-$) were separated and analyzed by immunoblotting (Figure 1B). Immunofluorescence of cross sections of the thoracic aorta with anti-αSMA and anti-HA and of *en face* images of the mesenteric artery stained with anti-PECAM1 and anti-HA show the EC specific expression of Cav-1-F92A (Figure 1C). Based on *en face* images, we estimate Cav-1-F92A is expressed in approximately 30% of EC in a mosaic pattern. Moreover, breeding of the Cdh5-tTA driver line[21] to a TetO7-GFP reporter mouse[22] (The Jackson Laboratory, #018913) documents the mosaic activation of GFP in a population of EC (Figure IB).

Blood pressure is lower in Cav-1-F92A transgenic animals and reversed by doxycycline treatment

Treatment of double transgenic animals with doxycycline (DOX; 2 mg/ml) in the drinking water leads to time dependent suppression of Cav-1-F92A expression at 3 and 7 days (Figure 2A) demonstrating DOX regulation of the transgene. Thus, single transgenic (control) and double transgenic (Cav-1-F92A) mice were implanted with telemetry devices for continuous monitoring of blood pressure. All mice were initially placed on water ("- DOX") and then switched to DOX drinking water ("+ DOX"). As seen in Fig. 2B, the systolic blood pressure of Cav-1-F92A mice increases significantly after 7 days treatment with DOX by shutting off the transgene (Figure 2A). Blood pressure increases at a rate of 0.028 mm Hg/hr upon switching the drinking water to DOX (Table I). The absence or presence of DOX had no effect on systolic pressures in control mice (Figure 2B). Although diastolic pressure changes were not significantly different, the trends were towards an increase (Figure IIA). These differences may relate to the mosaic nature of the transgene expression or the dominant effects of Cav-1 on systolic pressure[23]. Heart rates did not differ between the strains (Figure IIA). Treatment with L-NAME (1 mg/ml) leads to significantly increase of the systolic blood pressure of control and Cav-1-F92A mice (Figure 2C). The diastolic blood pressure changes in control and Cav-1-F92A mice significantly after 7 days treatment with L-NAME (Figure IIB). Heart rate decreases in control and Cav-1-F92A animals significantly after 7 days of L-NAME (Figure IIB).

Nitric oxide bioavailability is higher in Cav-1-F92A transgenic animals

The NO levels in whole blood were measured to assess if the Cav-1-F92A transgene influenced blood pressure through eNOS derived NO in vivo. Nitrosyl-hemoglobin (NO-Hb) was determined in venous blood by electron paramagnetic resonance (EPR). The three-line hyperfine spectrum at g = 2.01 with a splitting constant of ~ 17 G is specific for the 5-cordinated complex of NO• with hemoglobin as reported before[24] and can be used as a readout for eNOS derived NO as neither iNOS nor nNOS contribute to the formation of NO-

Hb under normal conditions[25]. Mice expressing the Cav-1-F92A mutant show a significant increase (165 %) of NO-Hb in their whole blood compared to WT (Figure 2D; representative traces in Figure III). As controls, venous blood from eNOS KO[26], eNOS S1176A (inactive) and eNOS S1176D (constitutively active) mice[27] (Figure IV) was measured. Isolated blood from eNOS KO (66 %) and the eNOS S1176A (41 %) mutant show significantly reduced NO-Hb levels, whereas eNOS S1176D have significantly higher (178 %) NO-Hb levels compared to the WT. NO activates soluble guanylate cyclase, the main NO receptor, and increases intracellular cGMP. cGMP activates protein kinase G (PKG) and the subsequent phosphorylation of vasodilator stimulated phosphoprotein (VASP) at Ser-239[28]. Analysis of the p-VASP/t-VASP ratio in aorta lysates reveal that mice expressing Cav-1-F92A have a significantly higher (131 %) phosphorylation status of Ser-239 of VASP compared to the WT controls (Figure 2E), thus indicating enhanced NO bioavailability.

Expression of Cav-1-F92A stabilizes endogenous Cav-2 and does not affect caveolae properties

Previous studies have shown that the genetic loss of Cav-1 destabilizes caveolin-2 (Cav-2) and to a lesser extent destabilizes the caveolin adaptor, Cavin-1[7, 9, 29]. Interestingly, Cav-1-F92A expression in EC enhances Cav-2 and Cavin-1 levels in whole lung lysates from transgenic mice (Figure 3A) demonstrating that Cav-1-F92A does not impair caveolae integrity, but likely stabilizes the protein complex. Additionally, Cav-2 stabilization as a readout of Cav-1 function was examined in immortalized Cav-1 KO MLEC transduced with adenoviral WT Cav-1 (AdCav-1 myc) or Cav-1-F92A (AdCav-1-F92A HA). Expression of similar levels of WT and Cav-1-F92A increased Cav-2 protein levels compared to AdGFP transduced cells (Figure 3B). To further assess the integrity of the Cav-1 enriched domains, the flotation of Cav-1 and Cav-1-F92A on sucrose gradients was performed. Both WT and Cav-1-F92A fractionated into buoyant membrane domains similarly (Figure 3C). Finally, transmission electron microscopy of WT and Cav-1 KO mouse embryonic fibroblasts (MEFs) infected with Ad Cav-1 or AdCav-1-F92A were examined and the morphology and numbers of caveolae/ length of plasma membrane were indistinguishable (Figure 3D) demonstrating that Cav-1 F92A can generate caveolae de novo.

Cav-1-F92A does not recapitulate the Cav-1 KO phenotypes

In addition to enhanced NO levels and systolic hypotension Cav-1 KO mice have mild pulmonary hypertension, fibrosis, and septal thickening[30, 31], and cardiac hypertrophy and dysfunction that worsens with age[7]. To examine if Cav-1-F92A mice exhibit any of these phenotypes, the lungs and hearts were histologically examined in aged mice (20 – 22 wk; Figure 4A). Cav-1-F92A mice did not show histological evidence of pulmonary or cardiac abnormalities or cardiac function differences as assessed by echocardiography in aged mice (Figure 4B and Table V). Echocardiographic analysis showed no differences between the two groups in left ventricle dimensions in diastole (LVD,d) or systole (LVD,s) thickness of the intraventricular septum wall (IVWS) or posterior wall (PW), parameters that were impaired in Cav-1 KO mice[32]. Due to persistent eNOS activation, Cav-1 KO mice exhibit increased tyrosine nitration of proteins that contributes to their pulmonary hypertension [31] however, tyrosine nitration of proteins was not different between the two strains of mice in

lungs and hearts (Figure VI). Finally, it is well described that Cav-1 KO mice show an increased phosphorylation of several downstream signaling pathways such as Akt and ERK1/2. Densitometric analysis of p-Akt/t-Akt and p-ERK/t-ERK ratios from shows no significant increase of either of these pathways (Figure 4C). Thus, the presence of Cav-1 F92A in endothelial cells containing endogenous Cav-1 is sufficient to lower SBP and increase circulating NO levels, however, Cav-1 F92A mice are phenotypically distinct from mice lacking Cav-1 globally.

DISCUSSION

This study was designed to answer three questions: (1) Is it possible to separate the formation of caveolae from downstream signaling in EC?; (2) Can a single point mutation in Cav-1 (F92A) disinhibit eNOS *in-vivo*?, and (3) Would the persistent expression of Cav-1-F92A lead to Cav-1 KO phenotypes? The Cdh5-driven, DOX-regulated expression of Cav-1-F92A was advantageous to a global knock-in strategy as it allows titration of Cav-1-F92A in the endothelium. Here we demonstrate that Cav-1-F92A uncouples the intracellular function of Cav-1 as a negative regulator of eNOS function from Cav-1 regulation of caveolae assembly. Prior work in Cav-1 KO mice could not distinguish between phenotypes due to flattening of caveolae versus phenotypes associated with altered intracellular signaling. Our results lend credence to the idea that the intracellular role of Cav-1 is separable from its role in caveolae biogenesis.

In our mouse model, the expression of the F92A Cav-1 transgene is suppressed within 7 days and during this period, the transgenic mice become normotensive again compared to the littermate single transgenic controls (i.e. there are no significant differences between control and Cav-1-F92A mice). In comparison to blood pressure measurements in Cav-1 KO animals, we did not detect an increase of the diastolic blood pressure[23], which is most likely to vascular and myocardial fibrosis and increased in vessel stiffness in the Cav-1 KO animals.

Double transgenic mice show significantly higher levels of both circulating NO-Hb *in-vivo* and phosphorylation of VASP-Ser-239 consistent with eNOS activation due to loss of endogenous Cav-1 suppression of eNOS (i.e. removal of inhibition). Despite the higher concentrations of nitric oxide in these animals, neither lungs, nor hearts displayed signs of fibrosis or hypertrophy akin to that seen in Cav-1 KO mice. Former studies have argued[3031] that excess nitric oxide can lead to S-nitrosylation of protein kinase-G, thereby facilitating pulmonary fibrosis. However, our study indicates that increased nitric oxide levels are not sufficient for the development of fibrosis in the heart and lungs, but could contribute to this detrimental effect if other Cav-1 functions have been dysregulated in mice lacking Cav-1.

Previous work in Cav-1 KO mice[23] found that these mice had lower systolic blood compared to controls and the heart rate was significantly higher. These changes were associated with increased NO bioavailability (measured by EPR and VASP phosphorylation). Despite these findings, it is well known, that Cav-1 KO animals exhibit both pulmonary and cardiac fibrosis[7, 30, 31] and altered signaling[7]. A robust readout of caveolae formation and function is measuring the Cav-2 protein level and to a lower extent

Cavin-1, as both proteins are in a stable protein complex with Cav-1, and the loss of Cav-1 genetically destabilizes endogenous Cav-2 and Cavin-1[7, 9, 29]. Whole lung or cardiac lysates show that EC expression of Cav-1-F92A indeed increased Cav-2 protein levels, suggesting that the point mutant F92A isoform did not disrupt the integrity of caveolae. Furthermore re-expression of either Cav-1 WT or Cav-1-F92A into Cav-1 KO MLECs led to a stabilization of Cav-2 protein similar to WT levels. Cav-1 or Cav-1-F92A proteins were distributed similarly on sucrose gradients and formed caveolae to the same extent indicating that the F92A point mutant of Cav-1 integrates into the plasma membrane caveolae in manner similar to the WT protein. Recent biophysical data shows that aa 102 – 134 are necessary to form the hairpin membrane domain of Cav-1[33, 34], and phenylalanine at position 92 is in a juxtamembrane cytoplasmic residue that will not affect the integration of aa 102–134 into the membrane.

In summary, our study shows that the expression of Cav-1-F92A leads to increases in NO release, without interfering with the formation of caveolae, indicating, that signaling and caveolae formation are independent functions of Cav-1 (Figure VII). These data complement data on the peptide cavnoxin (a cell penetrating caveolin peptide with contains 3 point mutations atT90A, T91A and F92A [20, 35]) and highlights the significance of F92 for the inhibitory action of Cav-1 on eNOS function. As neither the histological analysis nor the echocardiography showed any signs of cardiac hypertrophy or fibrosis in heart and lung, we surmise that prolonged therapeutic treatment with cavnoxin or similar acting small molecule could lead to a new class of therapeutics to improve endothelial dysfunction.

Supplementary Material

Refer to Web version on PubMed Central for supplementary material.

Acknowledgments

We thank Roger Babbitt for his invaluable technical assistance.

SOURCES OF FUNDING

This study was supported by the NIH (R01 HL64793, R01 HL61371, R01 HL081190, and P01 HL1070295), and the American Heart Association (Innovative Research Grant) to WCS. EPR studies were supported by the Department of Energy, Office of Basic Energy Sciences, Division of Chemical Sciences grant DE-FG02-05ER15646 (GWB and DJV). JRK was supported by the German Research Foundation (KR 4268/1-1). MYL was supported by the NIH (F32 HL119147). HV as part of the George M O'Brien Kidney Center at Yale was supported by the NIH (P30 DK079310).

Nonstandard Abbreviations and Acronyms

Cav-1	caveolin-1
Cav-2	caveolin-2
Cav-3	caveolin-3
eNOS	endothelial nitric oxide synthase
EPR	electron paramagnetic resonance

HA	hemagglutinin tag
Hb	hemoglobin
IVSW	intraventricular septum wall
LVD	d, left ventricle dimension in diastole
LVD	s, left ventricle dimension in systole
NO	nitric oxide
PW	posterior wall
Tg	transgene
tTA	tetracycline controlled transactivator
VASP	vasodilator-stimulated phosphoprotein

References

1. Frank PG, Pavlides S, Lisanti MP. Caveolae and transcytosis in endothelial cells: Role in atherosclerosis. Cell and tissue research. 2009; 335:41–47. [PubMed: 18688651]
2. Gratton J-P, Bernatchez P, Sessa WC. Caveolae and caveolins in the cardiovascular system. Circulation Research. 2004; 94:1408–1417. [PubMed: 15192036]
3. Yu J, Bergaya S, Murata T, Alp IF, Bauer MP, Lin MI, Drab M, Kurzchalia TV, Stan RV, Sessa WC. Direct evidence for the role of caveolin-1 and caveolae in mechanotransduction and remodeling of blood vessels. The Journal of clinical investigation. 2006; 116:1284–1291. [PubMed: 16670769]
4. Parton RG, Simons K. The multiple faces of caveolae. Nat Rev Mol Cell Biol. 2007; 8:185–194. [PubMed: 17318224]
5. Drab M, Verkade P, Elger M, Kasper M, Lohn M, Lauterbach B, Menne J, Lindschau C, Mende F, Luft FC, Schedl A, Haller H, Kurzchalia TV. Loss of caveolae, vascular dysfunction, and pulmonary defects in caveolin-1 gene-disrupted mice. Science. 2001; 293:2449–2452. [PubMed: 11498544]
6. Razani B, Engelman JA, Wang XB, Schubert W, Zhang XL, Marks CB, Macaluso F, Russell RG, Li M, Pestell RG, Di Vizio D, Hou H Jr, Kneitz B, Lagaud G, Christ GJ, Edelmann W, Lisanti MP. Caveolin-1 null mice are viable but show evidence of hyperproliferative and vascular abnormalities. J Biol Chem. 2001; 276:38121–38138. [PubMed: 11457855]
7. Murata T, Lin MI, Huang Y, Yu J, Bauer PM, Giordano FJ, Sessa WC. Reexpression of caveolin-1 in endothelium rescues the vascular, cardiac, and pulmonary defects in global caveolin-1 knockout mice. J Exp Med. 2007; 204:2373–2382. [PubMed: 17893196]
8. Lin MI, Yu J, Murata T, Sessa WC. Caveolin-1-deficient mice have increased tumor microvascular permeability, angiogenesis, and growth. Cancer research. 2007; 67:2849–2856. [PubMed: 17363608]
9. Fernandez-Hernando C, Yu J, Suarez Y, Rahner C, Davalos A, Lasuncion MA, Sessa WC. Genetic evidence supporting a critical role of endothelial caveolin-1 during the progression of atherosclerosis. Cell metabolism. 2009; 10:48–54. [PubMed: 19583953]
10. Maniatis NA, Shinin V, Schraufnagel DE, Okada S, Vogel SM, Malik AB, Minshall RD. Increased pulmonary vascular resistance and defective pulmonary artery filling in caveolin-1−/− mice. American journal of physiology. Lung cellular and molecular physiology. 2008; 294:L865–873. [PubMed: 18192592]
11. Razani B, Rubin CS, Lisanti MP. Regulation of camp-mediated signal transduction via interaction of caveolins with the catalytic subunit of protein kinase a. J Biol Chem. 1999; 274:26353–26360. [PubMed: 10473592]

12. Yamamoto M, Toya Y, Jensen RA, Ishikawa Y. Caveolin is an inhibitor of platelet-derived growth factor receptor signaling. Exp Cell Res. 1999; 247:380–388. [PubMed: 10066366]
13. Hagiwara M, Shirai Y, Nomura R, Sasaki M, Kobayashi K, Tadokoro T, Yamamoto Y. Caveolin-1 activates rab5 and enhances endocytosis through direct interaction. Biochemical and biophysical research communications. 2009; 378:73–78. [PubMed: 19013132]
14. Garcia-Cardena G, Martasek P, Masters BS, Skidd PM, Couet J, Li S, Lisanti MP, Sessa WC. Dissecting the interaction between nitric oxide synthase (nos) and caveolin. Functional significance of the nos caveolin binding domain in vivo. J Biol Chem. 1997; 272:25437–25440. [PubMed: 9325253]
15. Garcia-Cardena G, Oh P, Liu J, Schnitzer JE, Sessa WC. Targeting of nitric oxide synthase to endothelial cell caveolae via palmitoylation: Implications for nitric oxide signaling. Proc Natl Acad Sci U S A. 1996; 93:6448–6453. [PubMed: 8692835]
16. Ju H, Zou R, Venema VJ, Venema RC. Direct interaction of endothelial nitric-oxide synthase and caveolin-1 inhibits synthase activity. J Biol Chem. 1997; 272:18522–18525. [PubMed: 9228013]
17. Garcia-Cardena G, Fan R, Stern DF, Liu J, Sessa WC. Endothelial nitric oxide synthase is regulated by tyrosine phosphorylation and interacts with caveolin-1. J Biol Chem. 1996; 271:27237–27240. [PubMed: 8910295]
18. Gratton JP, Fontana J, O'Connor DS, Garcia-Cardena G, McCabe TJ, Sessa WC. Reconstitution of an endothelial nitric-oxide synthase (enos), hsp90, and caveolin-1 complex in vitro. Evidence that hsp90 facilitates calmodulin stimulated displacement of enos from caveolin-1. J Biol Chem. 2000; 275:22268–22272. [PubMed: 10781589]
19. Bernatchez PN, Bauer PM, Yu J, Prendergast JS, He P, Sessa WC. Dissecting the molecular control of endothelial no synthase by caveolin-1 using cell-permeable peptides. Proc Natl Acad Sci U S A. 2005; 102:761–766. [PubMed: 15637154]
20. Bernatchez P, Sharma A, Bauer PM, Marin E, Sessa WC. A noninhibitory mutant of the caveolin-1 scaffolding domain enhances enos-derived no synthesis and vasodilation in mice. The Journal of clinical investigation. 2011; 121:3747–3755. [PubMed: 21804187]
21. Sun JF, Phung T, Shiojima I, Felske T, Upalakalin JN, Feng D, Kornaga T, Dor T, Dvorak AM, Walsh K, Benjamin LE. Microvascular patterning is controlled by fine-tuning the akt signal. Proceedings of the National Academy of Sciences of the United States of America. 2005; 102:128–133. [PubMed: 15611473]
22. Krestel HE, Mayford M, Seeburg PH, Sprengel R. A gfp-equipped bidirectional expression module well suited for monitoring tetracycline-regulated gene expression in mouse. Nucleic acids research. 2001; 29:E39. [PubMed: 11266574]
23. Desjardins F, Lobysheva I, Pelat M, Gallez B, Feron O, Dessy C, Balligand JL. Control of blood pressure variability in caveolin-1-deficient mice: Role of nitric oxide identified in vivo through spectral analysis. Cardiovascular research. 2008; 79:527–536. [PubMed: 18349137]
24. Jaszewski AR, Fann YC, Chen YR, Sato K, Corbett J, Mason RP. Epr spectroscopy studies on the structural transition of nitrosyl hemoglobin in the arterial-venous cycle of deano-treated rats as it relates to the proposed nitrosyl hemoglobin/nitrosothiol hemoglobin exchange. Free radical biology & medicine. 2003; 35:444–451. [PubMed: 12899946]
25. Dikalov S, Fink B. Esr techniques for the detection of nitric oxide in vivo and in tissues. Methods in enzymology. 2005; 396:597–610. [PubMed: 16291267]
26. Shesely EG, Maeda N, Kim HS, Desai KM, Krege JH, Laubach VE, Sherman PA, Sessa WC, Smithies O. Elevated blood pressures in mice lacking endothelial nitric oxide synthase. Proc Natl Acad Sci U S A. 1996; 93:13176–13181. [PubMed: 8917564]
27. Schleicher M, Yu J, Murata T, Derakhshan B, Atochin D, Qian L, Kashiwagi S, Di Lorenzo A, Harrison KD, Huang PL, Sessa WC. The akt1-enos axis illustrates the specificity of kinase-substrate relationships in vivo. Sci Signal. 2009; 2:ra41. [PubMed: 19654415]
28. Oelze M, Mollnau H, Hoffmann N, Warnholtz A, Bodenschatz M, Smolenski A, Walter U, Skatchkov M, Meinertz T, Münzel T. Vasodilator-stimulated phosphoprotein serine 239 phosphorylation as a sensitive monitor of defective nitric oxide/cgmp signaling and endothelial dysfunction. Circulation Research. 2000; 87:999–1005. [PubMed: 11090544]

29. Davalos A, Fernandez-Hernando C, Sowa G, Derakhshan B, Lin MI, Lee JY, Zhao H, Luo R, Colangelo C, Sessa WC. Quantitative proteomics of caveolin-1-regulated proteins: Characterization of polymerase i and transcript release factor/cavin-1 in endothelial cells. Mol Cell Proteomics. 2010; 9:2109–2124. [PubMed: 20585024]

30. Wunderlich C, Schmeisser A, Heerwagen C, Ebner B, Schober K, Braun-Dullaeus RC, Schwencke C, Kasper M, Morawietz H, Strasser RH. Chronic nos inhibition prevents adverse lung remodeling and pulmonary arterial hypertension in caveolin-1 knockout mice. Pulmonary pharmacology & therapeutics. 2008; 21:507–515. [PubMed: 18226570]

31. Zhao YY, Zhao YD, Mirza MK, Huang JH, Potula HH, Vogel SM, Brovkovych V, Yuan JX, Wharton J, Malik AB. Persistent enos activation secondary to caveolin-1 deficiency induces pulmonary hypertension in mice and humans through pkg nitration. The Journal of clinical investigation. 2009; 119:2009–2018. [PubMed: 19487814]

32. Krieger MH, Di Lorenzo A, Teutsch C, Kauser K, Sessa WC. Telmisartan regresses left ventricular hypertrophy in caveolin-1-deficient mice. Laboratory investigation; a journal of technical methods and pathology. 2010; 90:1573–1581.

33. Lee J, Glover KJ. The transmembrane domain of caveolin-1 exhibits a helix-break-helix structure. Biochimica et biophysica acta. 2012; 1818:1158–1164. [PubMed: 22240009]

34. Rui H, Root KT, Lee J, Glover KJ, Im W. Probing the u-shaped conformation of caveolin-1 in a bilayer. Biophysical journal. 2014; 106:1371–1380. [PubMed: 24655512]

35. Sharma A, Sellers S, Stefanovic N, Leung C, Tan SM, Huet O, Granville DJ, Cooper ME, de Haan JB, Bernatchez P. Direct enos activation provides atheroprotection in diabetes-accelerated atherosclerosis. Diabetes. 2015

Novelty and Significance

What Is Known?

- Caveolae are enriched in endothelial cells and serve as reservoirs for membrane expansion and mechanosignaling.
- Caveolin-1 (Cav-1), a coat protein for caveolae, is essential for caveolae formation and suppression of nitric oxide (NO) release.

What New Information Does This Article Contribute?

- A mutant of Cav-1 promotes hypotension.
- Hypotension is linked to increases in NO levels in blood and tissue.

Here we show that mutant Cav-1 leads to increases in NO bioavailability in vivo supporting the idea that antagonizing the Cav-1/endothelial nitric oxide synthase interaction can improve endothelial function.

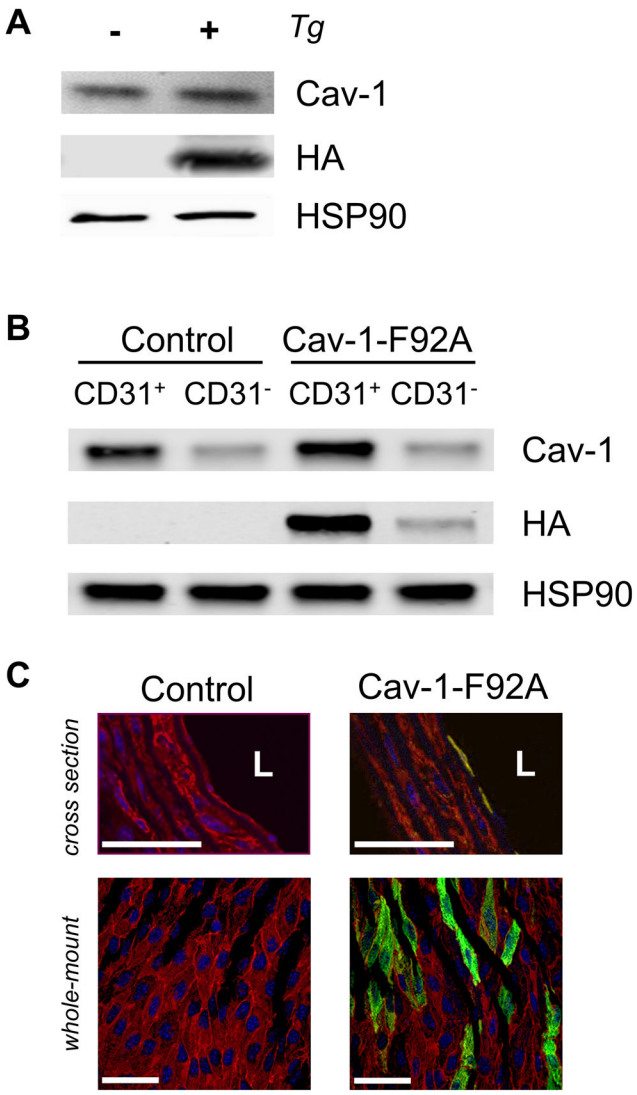

Figure 1. Expression of the Cav-1-F92A-HA transgene

A, Whole lung protein from control and Cav-1-F92A mice was analyzed for the expression of the transgene. B, MLECs were isolated with CD31-dynabeads. The fraction bound ($CD31^+$) and the non-bound fraction ($CD31^-$) was separated and immunoblotted for HA. The endothelial specific protein VECAD was used as a marker for the enrichment of endothelial cells by using the CD31-beads. C, Top panel, Cross sections of the thoracic aorta. Sections were stained for the nucleus (blue), α-SMA (red) and HA (green) [L, lumen]. Bottom panel, Whole-mount staining of mesenteric artery. En-face preparations were stained for the nucleus (blue), PECAM-1 (red) and HA (green). Scale bars are 50 μm.

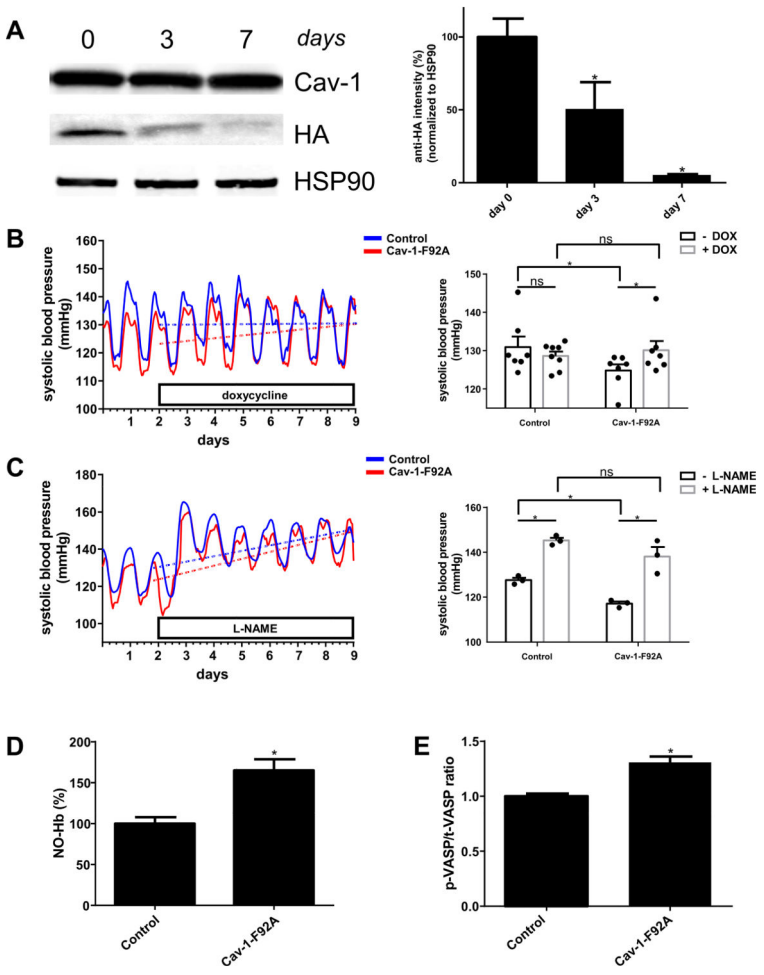

Figure 2. Effects of suppression of Cav-1-F92A-HA expression and nitric oxide measurements

A, Left panel, Whole lung protein from double transgenic mice was analyzed for the expression of the transgene at day 0, day 3 and day 7 after treatment with doxycycline (2 mg/ml) with 5 % sucrose in the drinking water. Each time point was repeated in three animals. Right panel, Densitometry analysis of the HA intensity and the HSP90 loading control. B, Left panels, Averaged systolic blood pressure from 8 control and 8 Cav-1-F92A animals. The first two days baseline was recorded, before drinking water was switched to doxycycline (2 mg/ml) with 5 % sucrose. Dotted lines show the changes of the systolic blood pressure (slopes of the curves are listed in Table I). Right panels, bar graph presentation of the same results. The bars present the average systolic blood pressure without and with doxycycline. C, Left panels, Averaged systolic blood pressure from 3 control and 3 Cav-1-F92A animals. The first two days baseline was recorded, before drinking water was switched to L-NAME (1 mg/ml). Dotted lines show the changes of the systolic blood pressure (slopes of the curves are listed in Table II). Right panels, bar graph presentation of the same results. The bars present the average systolic blood pressure without and with L-NAME. D, EPR-quantification of the peak to trough length of 4 mice each (representative traces are shown in Figure IV). E, Quantification of the p-VASP/t-VASP ratio (immunoblot is shown in Figure V).

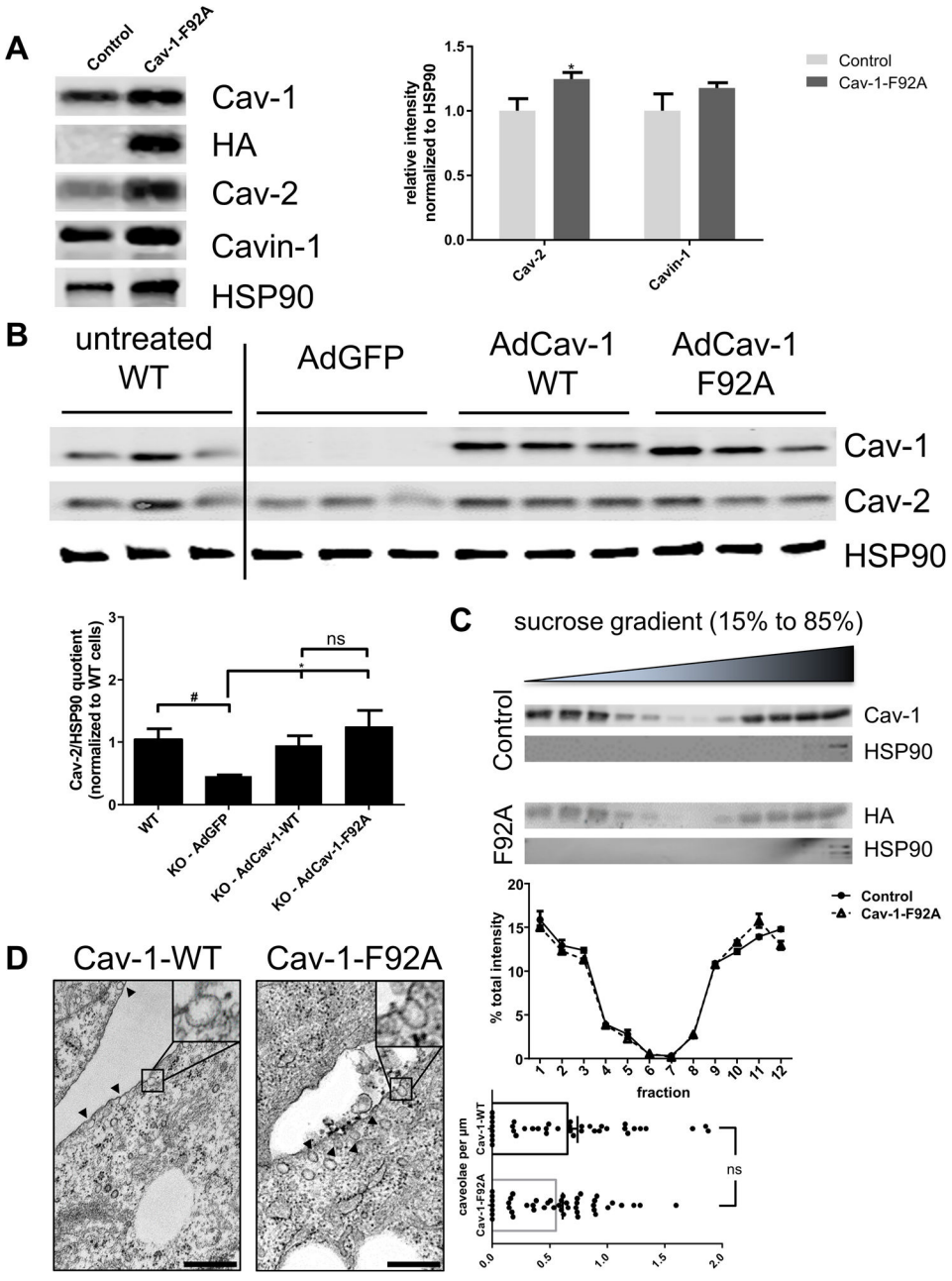

Figure 3. Stability of caveolae in the presence of Cav-1-F92A mutant

A, Left panel, Whole lung protein from single and double transgenic mice was analyzed for the expression of Cav-2 and Cavin-1. Cav-1 and HA immunoblotting as a control for the expression of the transgene. HSP90 was used as loading control. Right panel, Quantification of the relative intensity of Cav-2 and Cavin-1 normalized to HSP90. B, Adenoviral reconstitution of immortalized Cav-1 KO MLECs with either GFP, Cav-1 WT or Cav-1-F92A mutant. Immortalized WT cells are loaded as control for the expected expression level of Cav-1 and Cav-2. Cav-2 immunoblotting as a readout for the stability of caveolae. C, Top panel, Immunoblot analysis of Cav-1 (WT, endogenous) and (HA, transgene) of the sucrose

gradient fractions. HSP90 was used as marker for bulk fractions. Lower panel, Quantification of the immunoblot represented as % band intensity per fraction. D, TEM images for Cav-1 KO MEFs adenoviral reconstituted with WT or Cav-1-F92A mutant. Scale bar is 500 nm. At least 35 individual images were analyzed per group for the quantification of caveolae/μm of plasma membrane.

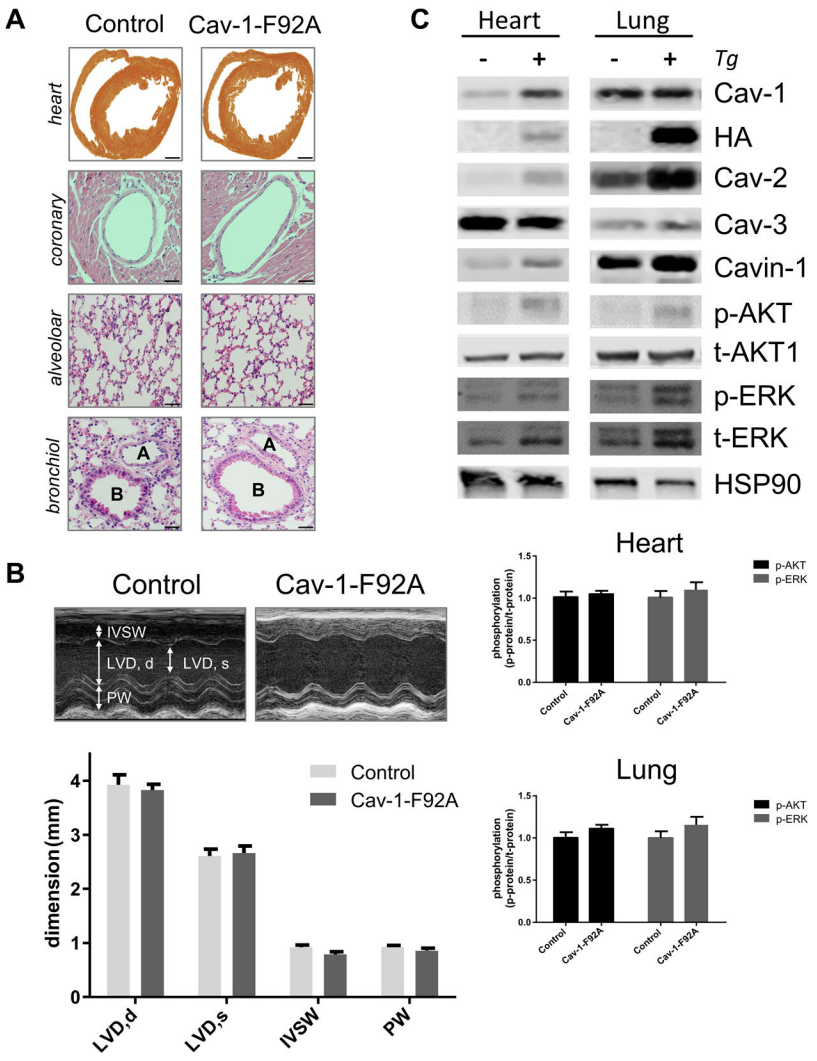

Figure 4. Histology, Echocardiography and Signaling

A, Histology of single (WT) and double transgenic (WT + Tg) mice. First panel, gross morphology of heart cross section through the ventricles. Second panel, Wall thickness of main coronary arteries. Third panel, Lung alveolar area. Fourth panel, Lung large bronchioles (B) and arteries (A). Scale bars: first panel: 1 mm, second to fourth panel: 200 μm. B, Echocardiography. Top panel, Representative M-mode images. Bottom panel, Quantification of the left ventricle diameter in diastole (LVD,d) and systole (LVD,s), the thickness of the intraventricular septum wall (IVSW) and the posterior wall (PW). Bar graph present the mean and the SEM for 5 WT and 5 WT + Tg animals. C, Signaling in heart and lung. Top panel shows representative immunoblots. Bottom panel shows the quantification for Akt and ERK activation by measuring the phospho/total ratio.